



Chaotic scattering of two identical point vortex pairs revisited

Tophøj, Laust Emil Hjerrild; Aref, Hassan

Published in:
Physics of Fluids

Link to article, DOI:
[10.1063/1.2974830](https://doi.org/10.1063/1.2974830)

Publication date:
2008

Document Version
Publisher's PDF, also known as Version of record

[Link back to DTU Orbit](#)

Citation (APA):
Tophøj, L. E. H., & Aref, H. (2008). Chaotic scattering of two identical point vortex pairs revisited. *Physics of Fluids*, 20(9), 093605. <https://doi.org/10.1063/1.2974830>

General rights

Copyright and moral rights for the publications made accessible in the public portal are retained by the authors and/or other copyright owners and it is a condition of accessing publications that users recognise and abide by the legal requirements associated with these rights.

- Users may download and print one copy of any publication from the public portal for the purpose of private study or research.
- You may not further distribute the material or use it for any profit-making activity or commercial gain
- You may freely distribute the URL identifying the publication in the public portal

If you believe that this document breaches copyright please contact us providing details, and we will remove access to the work immediately and investigate your claim.

Chaotic scattering of two identical point vortex pairs revisited

Laust Tophøj¹ and Hassan Aref^{1,2}

¹Center for Fluid Dynamics, Technical University of Denmark, Lyngby DK-2800, Denmark

²Department of Engineering Science and Mechanics, Virginia Tech, Blacksburg, Virginia 24061, USA

(Received 5 May 2008; accepted 12 June 2008; published online 11 September 2008)

A new numerical exploration suggests that the motion of two vortex pairs, with constituent vortices all of the same absolute circulation, displays chaotic scattering regimes. The mechanisms leading to chaotic scattering are different from the “slingshot effect” identified by Price [Phys. Fluids A **5**, 2479 (1993)] and occur in a different region of the four-vortex phase space. They may, in many cases, be understood by appealing to the solutions of the three-vortex problem obtained by merging two like-signed vortices into one of twice the strength and by assuming that the four-vortex problem has unstable periodic solutions similar to those seen in the thereby associated three-vortex problems. The integrals of motion, linear impulse and Hamiltonian are recast in a form appropriate for vortex pair scattering interactions that provides constraints on the parameters characterizing the outgoing vortex pairs in terms of the initial conditions. © 2008 American Institute of Physics.

[DOI: 10.1063/1.2974830]

I. INTRODUCTION

In an analytical and numerical study, Eckhardt and Aref¹ considered the scattering problem for two point vortex pairs. When the two-vortex pairs had circulations, $\pm\Gamma$ and $\pm\Gamma'$, with Γ and Γ' close in magnitude but not equal, an interesting hierarchical scattering dynamics was observed. The *scattering time* has an extremely complex structure with several plateaus separated by sharp jumps. The two incoming pairs first become dissociated into non-neutral pairs $(\Gamma, -\Gamma')$ and $(-\Gamma, \Gamma')$. The non-neutral pairs move on large circles and, when they encounter one another again, either scatter or recombine into the original $\pm\Gamma$ and $\pm\Gamma'$ pairs. When the latter happens, the scattering process is over and the two pairs depart the scattering region for infinity. However, the number of times the non-neutral pairs meet and scatter, afterward going for another loop, depends sensitively on the initial conditions, i.e., on the values of the known integrals, impulse, and energy. It is this sensitive variation that leads to the chaotic scattering and the jumps and plateaus in the scattering time as a function of impact parameter. The *scattering angle*, measured as the deflection between directions of motion for an incoming and outgoing pair, also showed very complex structure although it was not “quantized” in the same way as the scattering time. The reader is referred to Ref. 1 for more background and further details. This study provided one of the first examples of chaotic scattering, or “chattering” as it was also called, in a few-degrees-of-freedom dynamical system. The phenomenon had previously been suggested by preliminary numerical computations by Manakov and Shchur.² Some high precision calculations by Zawadzki, showing the real-space complexity of the two-pair scattering process, were later published in Ref. 3. While there are serious limitations to how much of this behavior is accessible experimentally with real vortices in an ordinary fluid, the basic exchange-of-partners mechanism has been beautifully illustrated.⁴ The first two interactions have even

been observed,⁵ but after that the vortices begin to decay, and the multiplicity of scatterings necessary for chaos probably cannot be observed in an ordinary fluid. Experiments in superfluids or analog experiments in plasmas have, so far as we know, not been attempted.

Although the chaos was observed to increase as Γ' and Γ became more nearly equal, the limiting case $\Gamma=\Gamma'$, surprisingly, appeared much more regular. (This statement is explained in more detail and quantified in Ref. 1 to which the reader is referred.) Certainly, the exchange of partners and the formation of non-neutral pairs upon interaction would be absent as a mechanism in the limit $\Gamma=\Gamma'$, but other mechanisms might arise. If so, however, these regimes were not readily apparent numerically. A continuous symmetry of the Hamiltonian for all circulations of the same magnitude was noted, and it was speculated whether this symmetry would lead to an additional integral of the motion. On balance, however, the relative regularity of the case of four vortices with circulations of equal absolute magnitude was left as a puzzle at the end of Ref. 1.

In 1993 Price⁶ considered the case of two identical pairs moving initially toward one another on parallel lines, where one pair was much larger, and so much slower, than the other. The smaller, faster-moving pair was aimed at one of the constituent vortices of the larger pair and would thus encounter it first in, essentially, a three-vortex interaction. An event approximating pair-single-vortex scattering would then occur. This three-vortex system and dynamics is integrable, and the scattering can be calculated in full detail.⁷ The outcome of a pair-single-vortex scattering event is that a pair of equal separation to the incoming pair exits from the scattering region (except for two singular values of the impact parameter). The outgoing pair may consist of the same two vortices that entered the three-vortex scattering region, in which case we call the process *direct scattering*. Alternatively, an *exchange scattering* may take place wherein the exiting pair contains the target vortex as one of its constitu-

ents, while one of the vortices of the incoming pair is left behind. Close to the two singular values of the impact parameter, where asymptotic trapping of all three vortices into a relative equilibrium takes place, and where one crosses over from direct to exchange scattering, the direction of the outgoing pair relative to that of the incoming pair changes rapidly with impact parameter, so large deflections are possible. If, as it exits from the first scattering, the outgoing small pair, regardless of composition, is headed for the second vortex of the large pair, a second three-vortex scattering process may take place. For certain initial conditions several such motions of the small pair, as it “bounces” back and forth between the vortices of the large pair, may take place (although the vortices of the large pair may, in fact, be exchanged with a vortex of the small pair upon one or more of these scatterings). Price⁶ referred to this as the “slingshot mode” and he showed by numerical calculations that it leads to chaotic scattering. This, in principle, resolved the problem left open in Ref. 1 and restated in Ref. 3: The system of two identical vortex pairs is not integrable, and a form of chaotic scattering can take place.

We have reexamined this problem by numerical simulation. We find that more conventional chaotic scattering processes may also take place when two identical vortex pairs—identical both as regards vortex strengths and initial separations—are launched at one another such that the linear momentum is nonzero. An essential element of the process is that two of the like-signed vortices, either negative or positive, come together so closely that they form a bound state for some time, around which the other two like-signed vortices orbit. The dynamics of the four vortices resembles the dynamics of the three-vortex problem $(\Gamma, \Gamma, -2\Gamma)$, which has again been integrated in detail.^{8,9} The four-vortex system follows this quasi-three-vortex motion for some time, eventually departing from it, maybe switching to another quasi-three-vortex motion, but ultimately reassembling into two neutral pairs that then depart for infinity. The length of time that the four-vortex system remains close to such quasi-three-vortex motions varies sensitively with the initial conditions and this variation leads to chaotic scattering. This paper contains an elaboration of this brief statement and illustrates it by several examples obtained numerically. Analysis of bounds on the vortex scattering process resulting from the integrals of motion is also provided. We have also explored scattering of two pairs with identical circulations when the separations of the vortices in the two pairs are not identical, but where the ratio of separations is still small compared to the ratios in Price’s study.⁶ Here also chaotic scattering occurs and appeal to the dynamics in an associated three-vortex problem is illuminating.

We conclude this section by stating the governing equations for the problem under consideration. There are four point vortices at positions z_1, z_2, z_3 , and z_4 in the complex plane. Vortices 1 and 3 have circulation $+\Gamma$ and vortices 2 and 4 have circulation $-\Gamma$. The equations of motion are

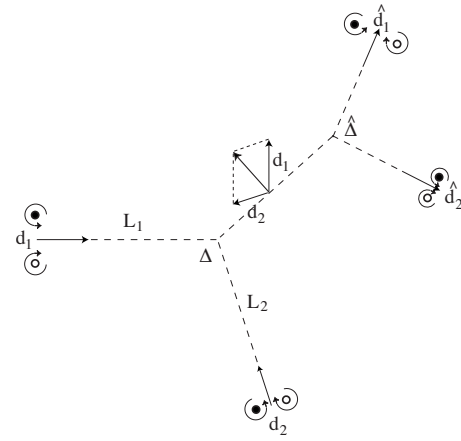


FIG. 1. Schematic of the scattering of two vortex pairs. The initial conditions [Eqs. (3) and (3’)] are shown as well as the scattering axis (defined in the text) and the outgoing pairs.

$$\frac{dz_1^*}{dt} = \frac{\Gamma}{2\pi i} \left[-\frac{1}{z_1 - z_2} + \frac{1}{z_1 - z_3} - \frac{1}{z_1 - z_4} \right], \quad (1a)$$

$$\frac{dz_2^*}{dt} = \frac{\Gamma}{2\pi i} \left[\frac{1}{z_2 - z_1} + \frac{1}{z_2 - z_3} - \frac{1}{z_2 - z_4} \right], \quad (1b)$$

$$\frac{dz_3^*}{dt} = \frac{\Gamma}{2\pi i} \left[\frac{1}{z_3 - z_1} - \frac{1}{z_3 - z_2} - \frac{1}{z_3 - z_4} \right], \quad (1c)$$

$$\frac{dz_4^*}{dt} = \frac{\Gamma}{2\pi i} \left[\frac{1}{z_4 - z_1} - \frac{1}{z_4 - z_2} + \frac{1}{z_4 - z_3} \right]. \quad (1d)$$

The asterisk denotes complex conjugation. This dynamical system is Hamiltonian, i.e., Eqs. (1a)–(1d) may be written as

$$\Gamma \frac{dz_\alpha^*}{dt} = 2i \frac{\partial H}{\partial z_\alpha}, \quad \alpha = 1, 3; \quad -\Gamma \frac{dz_\alpha^*}{dt} = 2i \frac{\partial H}{\partial z_\alpha}, \quad \alpha = 2, 4, \quad (2a)$$

where

$$H = \frac{\Gamma^2}{4\pi} \log \left| \frac{(z_1 - z_2)(z_1 - z_4)(z_2 - z_3)(z_3 - z_4)}{(z_1 - z_3)(z_2 - z_4)} \right|. \quad (2b)$$

We are concerned with solutions to this system when the initial conditions consist of two vortex pairs, 12 and 34, of comparable size, which are initially separated by distances much larger than the sizes of the pairs. Such initial configurations lead to vortex pair scattering.

II. NUMERICAL SCATTERING EXPERIMENTS

Let us parametrize the initial condition in the following way: We start from two vortex pairs with strengths $\pm\Gamma$ and separations d_1 and d_2 , respectively. Consider the centers of the two vortex pairs to be at a large distance from the origin, i.e., that the constituent vortices have coordinates of the form $(L_1, \pm d_1/2)$, respectively $(L_2, \pm d_2/2)$. Now turn the first pair through an angle θ_1 , the second through an angle θ_2 . See the lower left hand portion of Fig. 1. The initial positions of the vortices in the first pair may then be written as

$$\begin{aligned}
+\Gamma: & \left(L_1 \cos \theta_1 + \frac{d_1}{2} \sin \theta_1, L_1 \sin \theta_1 - \frac{d_1}{2} \cos \theta_1 \right), \\
-\Gamma: & \left(L_1 \cos \theta_1 - \frac{d_1}{2} \sin \theta_1, L_1 \sin \theta_1 + \frac{d_1}{2} \cos \theta_1 \right).
\end{aligned} \quad (3)$$

Similarly, the vortices in the second pair are at

$$\begin{aligned}
+\Gamma: & \left(L_2 \cos \theta_2 + \frac{d_2}{2} \sin \theta_2, L_2 \sin \theta_2 - \frac{d_2}{2} \cos \theta_2 \right), \\
-\Gamma: & \left(L_2 \cos \theta_2 - \frac{d_2}{2} \sin \theta_2, L_2 \sin \theta_2 + \frac{d_2}{2} \cos \theta_2 \right).
\end{aligned} \quad (3')$$

The values of the integrals, linear and angular impulse, for this initial condition are

$$\begin{aligned}
X + iY &= \sum_{\alpha=1}^4 \Gamma_{\alpha} (x_{\alpha} + iy_{\alpha}) \\
&= \Gamma (d_1 \sin \theta_1 + d_2 \sin \theta_2) \\
&\quad - i\Gamma (d_1 \cos \theta_1 + d_2 \cos \theta_2), \\
I &= \sum_{\alpha=1}^4 \Gamma_{\alpha} (x_{\alpha}^2 + y_{\alpha}^2) = 0.
\end{aligned} \quad (4)$$

The distances L_1 and L_2 do not enter these integrals. For a vortex system of the kind we are considering, where the net circulation is zero, one can change the value of the angular impulse by shifting the origin of coordinates. The value of the linear impulse is not changed by such a shift. We have clearly chosen our origin of coordinates such that $I=0$. In these coordinates the set of points for which $I=0$ is a line through the origin perpendicular to the linear impulse, i.e., the line with equation $xX + yY = 0$. Let us call this line the *scattering axis*.

The Hamiltonian equation (2b) is also conserved during the two pair scattering event. In the limit $L_1, L_2 \rightarrow \infty$, the Hamiltonian has the value $H = (\Gamma^2/4\pi) \log d_1 d_2$ for our chosen initial condition.

Figure 1 provides a schematic of the scattering between two vortex pairs based on numerical experiments. (A sampling of actual trajectories is in Fig. 2.) Two pairs of separations d_1 and d_2 , respectively, have been set on a collision course. There are three distinct phases of the scattering process: Impingement, interaction, and separation. During the impingement phase the two pairs propagate with minimal effect of their interaction, essentially along intersecting straight lines and essentially with the velocity of a vortex pair alone on the infinite plane. As they approach one another, a complex interaction phase takes place (we will discuss details of this process later) in which all four vortices orbit one another for some time. Ultimately, in the separation phase, two pairs emerge from this interaction (for almost all initial conditions) and propagate to infinity again essentially as two freely moving pairs on the infinite plane. During the interaction phase the four-vortex system may propagate for some considerable distance (see Fig. 2). As indicated in Fig.

1, let the outgoing pairs have separations \hat{d}_1 and \hat{d}_2 , respectively. Consider the perpendicular bisectors of the two outgoing pairs. They will, in general, intersect at some point relative to which the vortices in the outgoing pairs must again have coordinate formulas of the same form as the vortices in the incoming pairs, Eqs. (3) and (3'), except that the sense of the vortices is reversed such that the pairs propagate away from the interaction region. In particular, the point at which the outgoing pairs separate must also be on the aforementioned scattering axis. The vectors of length d_1 and d_2 , respectively, connecting negative to positive vortex in each incoming pair add up vectorially to the linear impulse (modulo a factor Γ). Hence, if we add these two vectors and draw the line perpendicular to the resultant through the point of impingement of the incoming pairs, we get the scattering axis. The point at which the two outgoing pairs separate must also be on this line, and the vector resultant of the separations pairwise in the outgoing pairs is the same as for the incoming pairs. This is all summarized in Fig. 1.

Let the corresponding polar angles for the outgoing pairs be $\hat{\theta}_1$ and $\hat{\theta}_2$. Conservation of X and Y then gives

$$d_1 \sin \theta_1 + d_2 \sin \theta_2 = -\hat{d}_1 \sin \hat{\theta}_1 - \hat{d}_2 \sin \hat{\theta}_2, \quad (5)$$

$$d_1 \cos \theta_1 + d_2 \cos \theta_2 = -\hat{d}_1 \cos \hat{\theta}_1 - \hat{d}_2 \cos \hat{\theta}_2,$$

while conservation of H tells us that

$$d_1 d_2 = \hat{d}_1 \hat{d}_2. \quad (6)$$

Squaring Eq. (5), adding, using Eq. (6), and setting $r = d_1/d_2$, $\Delta = \theta_1 - \theta_2$, we see that the quantity $M \equiv (X^2 + Y^2)/(2d_1 d_2 \Gamma^2)$, i.e.,

$$M = \frac{1}{2} \left(r + \frac{1}{r} \right) + \cos \Delta = \cosh(\log r) + \cos \Delta, \quad (7)$$

is invariant during the scattering. The second form may seem slightly artificial but the reason for writing M this way will become clear momentarily.

Equation (5) contains information about the direction of the linear impulse as well. Note that $X + iY = -i(d_1 e^{i\theta_1} + d_2 e^{i\theta_2})$. If we set

$$X + iY = |X + iY| e^{i\Phi} = \sqrt{2d_1 d_2 \Gamma^2} M e^{i\Phi}, \quad (8)$$

we have

$$\begin{aligned}
-(X + iY)^2/\Gamma^2 &= (d_1 e^{i\theta_1} + d_2 e^{i\theta_2})^2 \\
&= d_1^2 e^{i2\theta_1} + d_2^2 e^{i2\theta_2} + 2d_1 d_2 e^{i(\theta_1 + \theta_2)} \\
&= 2d_1 d_2 e^{i(\theta_1 + \theta_2)} \left[\frac{1}{2} \left(r e^{i\Delta} + \frac{1}{r} e^{-i\Delta} \right) + 1 \right] \\
&= 4d_1 d_2 e^{i(\theta_1 + \theta_2)} \cosh^2 \left(\frac{1}{2} \log r + i \frac{\Delta}{2} \right).
\end{aligned}$$

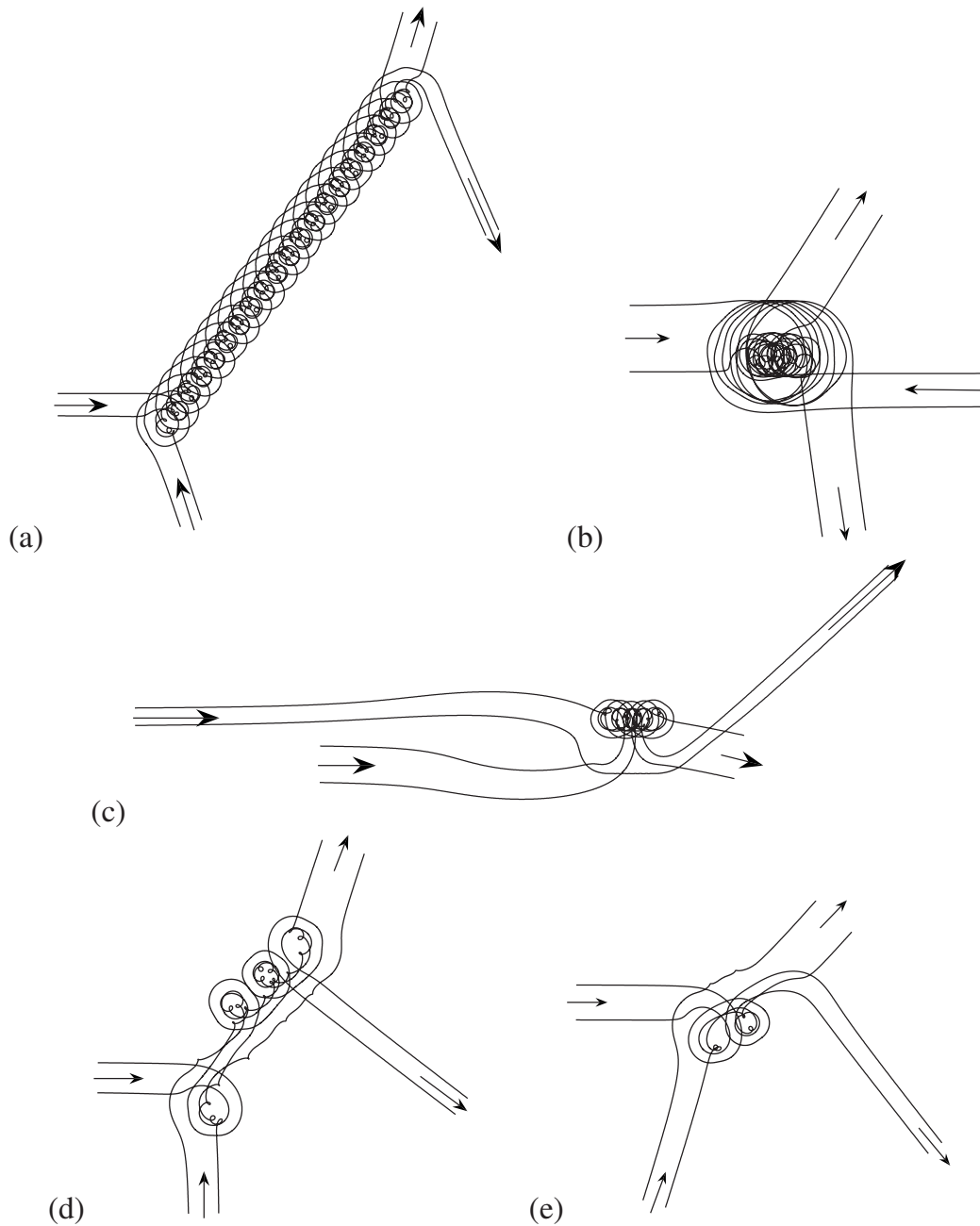


FIG. 2. Sample trajectories of two vortex pairs impinging on one another, scattering through an extended process, and finally separating into two pairs. In terms of the parameters defined in the text (a) corresponds to $(r, \Delta, \rho) = (1, -3\pi/5, 0.979, \dots)$, (b) $(2, \pi, 0.7745, \dots)$, (c) $(2, 0, 1.2551, \dots)$, (d) $(1, -\pi/2, 0.975, \dots)$, and (e) $(1.2, -2\pi/5, -0.152)$. The case shown in (a) is analyzed further in Fig. 5. For clarity, incoming and outgoing pairs are identified by arrows.

Thus, from $-(X+iY)^2/\Gamma^2 = 2d_1d_2Me^{i(2\Phi-\pi)}$, we have finally that

$$\Phi = \frac{\pi}{2} + \frac{1}{2}(\theta_1 + \theta_2) + \arg \left[\cosh \left(\frac{1}{2} \log r + i \frac{\Delta}{2} \right) \right] \quad (9)$$

must also be conserved during the collision process. Equations (7) and (9) connect $\log r$ and Δ before and after the scattering process. Equation (9) also involves the average of the two impingement angles (and for the exiting pairs the

average of the two angles into which they have been scattered).

If the separation ratio is unchanged by the scattering, $\hat{r} = r$ or $\hat{r} = 1/r$. Conservation of M then implies $\hat{\Delta} = \pm \Delta$. We can always choose to number the outgoing pairs so that $\hat{\Delta} = \Delta$. Using the conservation of Φ , this leads to $(\hat{\theta}_1, \hat{\theta}_2) = (\theta_1, \theta_2)$. The vortex pairs are thus essentially unaffected by the interaction, the only possible change being a finite displacement of the whole trajectory after the interaction. Note that for the integrable cases of collision of two pairs when

$X=Y=0$, the angle Φ is indeterminate so that its conservation is not a constraint. This is equivalent to $M=0$ which is only possible if $r=1$ and $\Delta=\pi$. It then follows that $\hat{r}=1$ and $\hat{\Delta}=\pi$ as well. This accommodates the solution wherein the two pairs exchange partners, which proceed to infinity along lines at right angles to the direction of propagation of the incoming pairs. For two pairs of different sizes with a common axis, the motion is integrable because of the symmetry. The resulting pairs, which still are symmetric with respect to the common axis, can either have $\hat{r}=r$ or $\hat{r}=1$ (see Ref. 1, Appendix B).

Scattering will most often result in a change in r . For example, the collision of equal-size pairs in Fig. 2(a) clearly produces outgoing pairs of unequal size. A complex intermediate interaction plays out, with all four vortices within close range of one another for a finite time. Different realizations of the interaction region, produced by varying initial conditions, are shown in the various panels of Fig. 2. The interaction region is along the scattering axis, and the points of impingement and separation of incoming and outgoing pairs, respectively, define the end points of this region. The length of the interaction region depends sensitively on the initial conditions in much the same way that the interaction sequence for unequal pairs showed sensitive dependence. This is a new mechanism for chaos in the scattering dynamics of two identical vortex pairs, quite distinct from the slingshot mechanism identified by Price,⁶ and more in keeping with the notion of a scattering event between two-vortex pairs than the slingshot mode. Taken together, this study and Price's work⁶ leave no doubt that the system of two identical vortex pairs is nonintegrable, and so resolve the issue left open in Ref. 1.

We note that one can have chaotic scattering even for $\Delta=\pi$ [head-on collision, Fig. 2(b)] and for $\Delta=0$ [tail-to-tail collision, Fig. 2(c)]. For a head-on collision, $\cos \hat{\Delta} \geq \cos \Delta = -1$. Hence, using Eq. (7) we get $\hat{r} + \hat{r}^{-1} \leq r + r^{-1}$, i.e., the ratio of separations for the outgoing pairs, \hat{r} , is bounded by the ratios of separations for the incoming pairs, d_1/d_2 and d_2/d_1 . These interactions, then, tend to *focus* the distribution of energy over length scales in the flow. Conversely, for tail-tail interactions, we have $\cos \Delta = 1 \geq \cos \hat{\Delta}$, so $\hat{r} + \hat{r}^{-1} \geq r + r^{-1}$, and \hat{r} is either larger than $\max\{d_1/d_2, d_2/d_1\}$ or smaller than $\min\{d_1/d_2, d_2/d_1\}$. These interactions, then, will tend to *disperse* energy over length scales of the flow.

In Fig. 2 we have shown the incoming and outgoing pairs by arrows. However, since the dynamics is reversible, one could equally well “read” these trajectory plots by switching final and initial pairs. This would correspond to reversing the signs of all vortex circulations and the direction of all arrows. In later plots we therefore drop the arrows, in effect capturing two scattering experiments in one diagram.

In order to do a sweep through different initial conditions, we proceed as follows: In place of the initial conditions given for the second pair, we use

$$\begin{aligned} +\Gamma: & \left[L_2 \cos \theta_2 + \left(\frac{d_2}{2} + \rho \right) \sin \theta_2, \right. \\ & \left. L_2 \sin \theta_2 - \left(\frac{d_2}{2} + \rho \right) \cos \theta_2 \right], \\ -\Gamma: & \left[L_2 \cos \theta_2 - \left(\frac{d_2}{2} - \rho \right) \sin \theta_2, \right. \\ & \left. L_2 \sin \theta_2 + \left(\frac{d_2}{2} - \rho \right) \cos \theta_2 \right], \end{aligned} \quad (10)$$

i.e., we have shifted the second vortex pair up or down along the y -axis by ρ before rotating it through the angle θ_2 . (Shifts down correspond to positive ρ ; shifts up to negative ρ .) Such a shift does not change the values of the components of the linear impulse, X or Y . However, the angular impulse is now $I=2\Gamma d_2 \rho$. A sweep in ρ may therefore be considered to be a sweep through various values of the angular impulse for fixed values of the linear impulse and the Hamiltonian. Note that since X and Y are unchanged, we will still have conservation of M [Eq. (7)] and of Φ [Eq. (9)].

A somewhat different interpretation arises by reasoning as follows: The velocities of free propagation of the two initial pairs are $v_1=\Gamma/2\pi d_1$ and $v_2=\Gamma/2\pi d_2$. Set $L_1=v_1 T$, $L_2=v_2 T$, where T is a large time interval. The initial conditions (10), which we are using in the sweep through different values of I , have shifted the vortices in the second pair by $\rho(\sin \theta_2, -\cos \theta_2)$ relative to Eqs. (3) and (3'). This means that the point of intersection of the two lines corresponding to freely propagating pairs has been shifted. A simple calculation gives that the “free flight” distances L_1 and L_2 from Eqs. (3) and (3') should be changed to $L'_1=L_1+\rho \csc \Delta$ and $L'_2=L_2+\rho \cot \Delta$, respectively. The time from initial launch of the vortex pairs until they impinge upon one another is thus changed by $2\pi\rho(d_1 \csc \Delta + d_2 \cot \Delta)/\Gamma$. At fixed d_1 , d_2 , and Δ , this delay is simply proportional to ρ .

When the two pairs scatter we can define various scattering angles: We could monitor the absolute angle between the direction of an outgoing pair and the direction of an incoming pair. The outgoing and incoming pairs may be made up of different vortices. We can both have interactions where the same two pairs enter and exit the scattering region, as well as interactions of the form $12+34 \rightarrow 14+23$ (using an easily understood notation). Interactions of the first kind will again be called direct scattering, interactions of the second kind exchange scattering. One should, therefore, look at the angle between the outgoing pair containing a given vortex and the incoming pair containing that same vortex. Alternatively—and this is the measure we have used—one can consider the value of $\Delta=\theta_1-\theta_2$ before and after collision.

The result of performing multiple numerical scattering “experiments” at many values of ρ , with an initial condition for which $\Delta=-3\pi/5$ and $r=d_1/d_2=1$, is shown in Fig. 3 (top panel). The abscissa shows ρ in units of the original, common vortex pair size d . The ordinate gives $\cos \hat{\Delta}$, the cosine of the angle difference between the outgoing pairs. We have used $L_1=L_2 \gg d$ and checked that the general nature of the

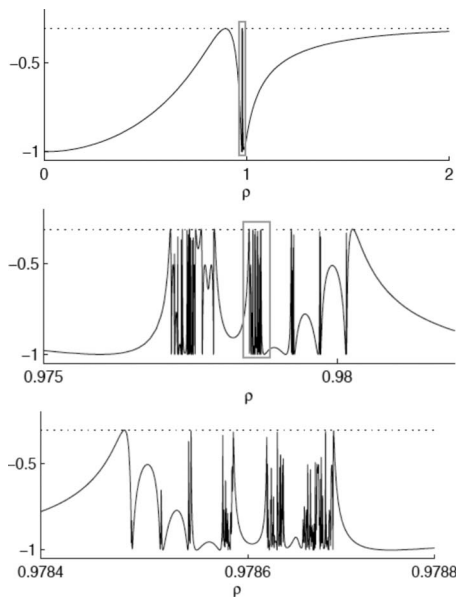


FIG. 3. The cosine of the scattering angle (angle between the two outgoing vortex pairs), $\cos \hat{\Delta}$, as a function of the parameter ρ , introduced in the text, which measures the angular impulse of the vortex system; ρ is measured in units of the common initial separation of the two identical incoming pairs. (Top panel) Scan of a larger range of ρ ; (middle panel) magnification of the region around $\rho=1$; and (bottom panel) further magnification showing more fine structures. The dotted line indicates the value of $\cos \Delta$ for the initial pairs, i.e., for $r=1$. In general, $\cos \hat{\Delta} < \cos \Delta$ and only reaches $\cos \Delta$ when the outgoing pairs are also identical.

results is independent of the specific values of L_1 and L_2 , although the exact positions of the various spikes in $\cos \hat{\Delta}$, to be discussed below, will, of course, vary slightly as these parameters are changed. Except for $\rho \approx 1$, the result of the scattering appears relatively featureless. When $|\rho| \gg 1$, the two pairs “miss” one another by a wide margin, and both continue along their straight line trajectories essentially unperturbed. In that limit, then, $\cos \hat{\Delta} = \cos \Delta = \cos(3\pi/5) = \frac{1}{4}(1 - \sqrt{5}) \approx -0.309$. This is the level shown by the horizontal dotted line. In general, we have $M = 1 + \cos \Delta = \frac{1}{2}(\hat{r} + \hat{r}^{-1}) + \cos \hat{\Delta} \geq 1 + \cos \hat{\Delta}$, where the hats refer to quantities after the scattering. Thus, $\cos \hat{\Delta} \leq \cos \Delta$, and the angle between the outgoing pairs must be at least as obtuse as the angle between the incoming pairs. This is clearly evident in the scattering process of Fig. 2(a). The peaks in $\cos \hat{\Delta}$ (Fig. 3) will thus, at best, reach the initial value of $\cos \Delta$.

If one probes the scattering diagram in Fig. 3 in a narrow band of ρ -values around $\rho=1$, the spike visible in the top panel of Fig. 3 reveals considerable fine structure. In the middle panel of Fig. 3 we have magnified a segment of the ρ -axis, $0.975 < \rho < 0.985$, indicated in the top panel by the thin gray rectangle. We see that what appeared as a single spike in the top panel resolves itself into a multitude of spikes. Many of these reach up to $\cos \Delta$, which, from the conservation of M during scattering, means that the outgoing pairs also have the same size, which must be equal to the common size of the incoming pairs by conservation of the Hamiltonian. In between these maxima we have additional structure in the scattering angle $\hat{\Delta}$. This process of selecting

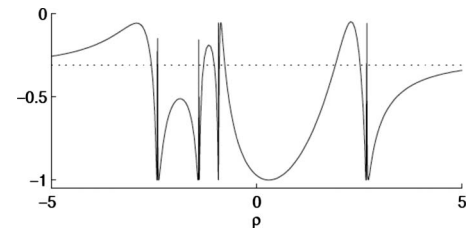


FIG. 4. The cosine of the scattering angle (angle between the two outgoing vortex pairs), $\cos \hat{\Delta}$, as a function of the parameter ρ , introduced in the text, for two incoming pairs with separations d and $2d$ ($r=2$); ρ is measured in units of d . The dotted line is again at $\cos \Delta$ for the initial pairs (and $\Delta = -3\pi/5$), but since $r=2$, the peaks in $\cos \hat{\Delta}$ can now reach higher as explained in the text.

and magnifying a piece of the ρ -interval may be repeated. The gray rectangle shown in the middle panel of Fig. 3 has been magnified in the bottom panel of Fig. 3, which now explores the interval of $0.9784 < \rho < 0.9788$. Again we see that the fine structure apparent in the middle panel of Fig. 3 continues to exist as we zoom in on smaller and smaller intervals of ρ . The curve continues to have fine structure as the ρ -interval is probed on finer and finer subintervals. This is the hallmark of chaotic scattering and is quite similar to what was observed in Refs. 1 and 3 and in other chaotic scattering problems.

The complexity of Fig. 3 can be understood in terms of the sample scattering process in Fig. 2(a). The length of the scattering process seen in this figure depends sensitively on the initial conditions, i.e., on ρ . In the chaotic scattering region, a change in ρ , however slight, can result in dramatic changes in the scattering process, making it either shorter or longer and altering the resulting scattering angle. One can also monitor the scattering time, i.e., the time between the initial encounter of the two pairs and their final separation. This diagnostic again shows sensitive dependence on the initial conditions. The scattering time as a function of ρ is not as dramatically quantized as it was for the case of two unequal pairs,¹ where each loop of two non-neutral pairs added a step in the scattering time. However, it does again have a ramified structure much as the scattering angle shown in Fig. 3. Furthermore, the structure in the scattering time corresponds to the structure in the scattering angle plot, further bolstering the argument that we are witnessing a chaotic scattering process.

We have also conducted scattering experiments with pairs of unequal separation in the initial condition. Figure 4 shows the $\cos \Delta$ diagnostic as a function of ρ for two incoming pairs with a separation ratio of $r=2$. There are now several peaks, each of which resolves into further fine structure if a segment of the ρ -interval is magnified. Conservation of M now yields $\frac{1}{2}(2 + \frac{1}{2}) + \cos \Delta \geq 1 + \cos \hat{\Delta}$ or $\cos \hat{\Delta} \leq \frac{1}{4} + \cos \Delta \approx -0.059$. This gives the height of the tallest peaks in Fig. 4, which occur when the outgoing pairs have equal size.

In order to obtain a better understanding of the motion depicted in Fig. 2(a), and how it might originate, we have explored the vortex trajectories in more detail. See the analogous study for the case of unequal pairs in Ref. 3. The results are shown in Fig. 5. The first panel [Fig. 5(a)] shows one

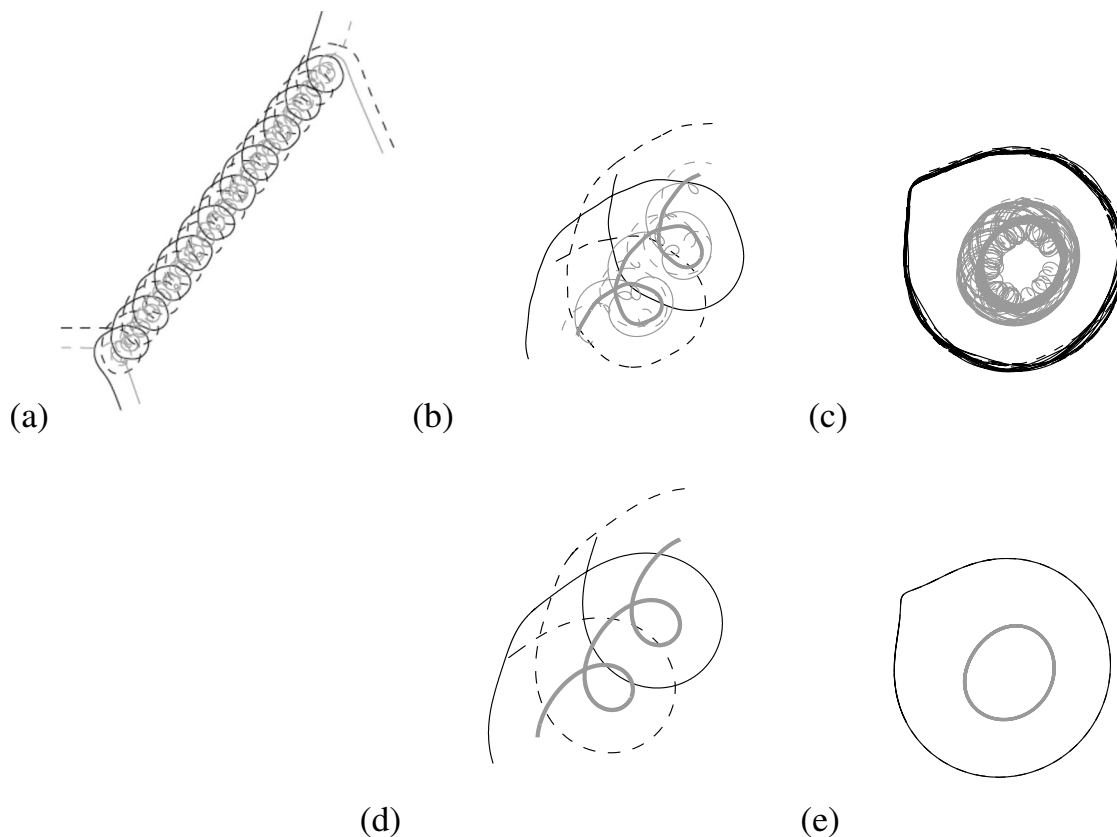


FIG. 5. (a) Trajectory from Fig. 2(a) with vortices identified, $r=1$, $\Delta=-3\pi/5$, and $\rho\approx 0.979$. (b) Detail of the trajectories of the four vortices with the trajectory of the midpoint of the two negative vortices superimposed. (c) Trajectories relative to a frame of reference translating with the mean velocity of the group. (d) Comparison trajectories to panel (b) for the system $(\Gamma, \Gamma, -2\Gamma)$. (e) Comparison to panel (c) for the system $(\Gamma, \Gamma, -2\Gamma)$.

incoming pair as solid black and gray lines, the other as dashed lines. Positive vortices are black, negative vortices are gray. We see, first of all, that an exchange scattering process has taken place. In Fig. 5(b) we have magnified a portion of the trajectories that appears to be repeated over and over. (We have also added a fifth “trajectory” as discussed in what follows.) We see that the two negative vortices move to the inside of the long structure seen in Figs. 2(a) and 5(a), and that the two positive vortices orbit on the outside of this structure. If we think of this bound state of the two negative vortices as equivalent to a single vortex of strength -2Γ , we may look to the integrable three-vortex problem $(\Gamma, \Gamma, -2\Gamma)$ for understanding. [The thicker solid gray curve that has been superimposed in Fig. 5(b) is the trajectory of $\frac{1}{2}(z_2+z_4)$.] In this problem there are regimes of motion similar to what is seen in Figs. 5(a) and 5(b). The trio of vortices propagates along, in a direction given by the total linear impulse, while the two positive vortices orbit one another and the stronger negative vortex. To illustrate this more clearly, we have subtracted out the mean translation velocity of the entire group in Fig. 5(c). The negative vortices are now clearly seen to orbit “on the inside” with the two positive vortices orbiting around them. To bolster this interpretation further, we have calculated trajectories for the three-vortex system $(\Gamma, \Gamma, -2\Gamma)$ starting from an initial condition produced as follows: While the four-vortex motion is undergoing the interactions seen in Fig. 5(a), we recorded the positions of the four vortices at some instant. We then took the

two positive vortices as vortices 1 and 2 of a three-vortex problem, and we took the location of the midpoint of the line connecting the two negative vortices as the location of vortex 3 of strength -2Γ . A calculation was then started for these three vortices and trajectory plots analogous to those in Figs. 5(b) and 5(c) were produced. These are shown in Figs. 5(d) and 5(e). The two positive vortices have trajectories that correspond well to those in the original four-vortex problem. The negative vortex of strength -2Γ has a trajectory that is very similar to the trajectory of $\frac{1}{2}(z_2+z_4)$ in the four-vortex problem. This comparison between three-vortex and four-vortex trajectories is quite convincing that, indeed, an intermediate state reminiscent of the periodic three-vortex motion is observed.

Hence, the qualitative explanation of the chaotic scattering is that the four-vortex system has unstable periodic orbits reminiscent of those in the naturally associated three-vortex problem, and that these can produce long term transients. We hypothesize that there is an infinity of such periodic orbits, continuously distributed in terms of the values of the integrals of motion, and that they can be accessed as the scattering parameter ρ is continuously varied. The point at which the four-vortex problem begins following the periodic orbit, and the point at which it again deviates from it, would be expected to depend sensitively on the initial conditions.

Generally, there are four possible regimes in the three-vortex problem $(\Gamma, \Gamma, -2\Gamma)$. In one the two positive vortices, 1 and 2, “pair up” and orbit as an entity with vortex 3 fol-

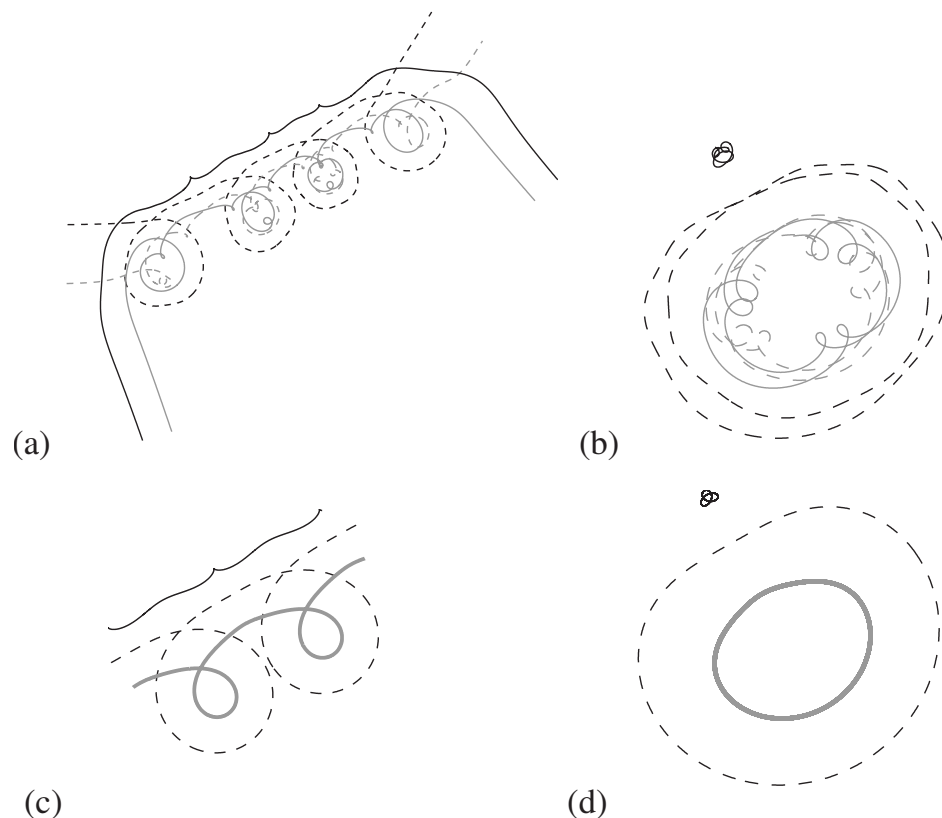


FIG. 6. (a) Trajectories with all vortices identified—a four-vortex motion that corresponds to the three-vortex problem $(\Gamma, \Gamma, -2\Gamma)$ in the regime $1+(23)$. (b) Trajectories relative to a frame of reference translating with the mean velocity of the group. (c) Comparison trajectories to panel (a) for the three-vortex system. (d) Comparison to panel (b) for the three-vortex system.

lowing along at some distance. We could write this as $(12)+3$. In another, one positive and one negative vortex pair up, say 1 and 3, and they orbit with vortex 2 following along. In this regime the vortex system has aspects of a vortex pair with one constituent being the bound state of vortices 1 and 3, the other being vortex 2. We could write this as $2+(13)$. Similarly, vortices 2 and 3 can pair up and vortex 1 then follows along at a distance, i.e., we would have $1+(23)$. Finally, no two vortices need to pair up and the vortices all interact at all times. We might call this the “collective regime.” See Refs. 8 and 9 for the derivation of these results. The motion in Fig. 5(d) and, hence, the four-vortex scattering process seen in Fig. 5(a) correspond to this collective regime.

The question then arises if the other three-vortex regimes mentioned are possible as intermediaries in a scattering process. Regime $(12)+3$ necessitates the simultaneous pairing of the two positive and the two negative vortices, and thus projects the four-vortex problem onto a two-vortex problem. We have only seen this happen for very short periods of time. However, the other two regimes—where one has the two negative vortices orbiting as, effectively, a single vortex of strength -2Γ , and this is “paired” with one of the positive vortices, leaving the last positive vortex to follow along at a distance—are more easily found. Figure 6 shows such an intermediate motion [and see also Figs. 2(d) and 2(e)]. One has to start with $r \neq 1$ and one has to find a propitious value of ρ . We used $r=2$, $\Delta=-3\pi/5$, and tuned the value of $\rho \approx 0.820$ to produce the trajectories in Fig. 6, which clearly

have the sought after features. We show the full scattering process in Fig. 6(a) with the vortex trajectories differentiated (the net process is a direct scattering), the motion with the mean translation velocity subtracted out in Fig. 6(b), the trajectories in the associated three-vortex problem $(\Gamma, \Gamma, -2\Gamma)$ started from simultaneous values of z_1 , z_3 , and $\frac{1}{2}(z_2+z_4)$ in Fig. 6(c), and the same three-vortex trajectories with the mean translation velocity subtracted out in Fig. 6(d).

Finally, to illustrate the richness of periodic solutions that the four-vortex problem can approach and follow for varying amounts of time, we show in Fig. 7 a trajectory plot produced for $r=2$, $\Delta=-3\pi/5$, and $\rho \approx 0.819$. In this case, we see that the bound motion of the four vortices starts out close to the three-vortex problem $(\Gamma, \Gamma, -2\Gamma)$ as before, but now in the mode $1+(23)$, then switches to a similar mode of the three-vortex problem $(2\Gamma, -\Gamma, -\Gamma)$. Then there is a brief period where it appears that the motion follows the integrable “leapfrogging” mode of two coaxial vortex pairs (see Ref. 1, where the historical Refs. 10 and 11 are discussed). We get one loop of the first three-vortex-like motion before the original vortex pairs depart for infinity. The net result of this lengthy interaction is a direct scattering process.

The various patterns of appearance of intermediate bound states could be labeled with letters as was done in Ref. 1, e.g., the regime numbers for the various associated three-vortex problems, supplemented by L for leapfrogging. Alternatively, the braids in three-dimensional space-time could be

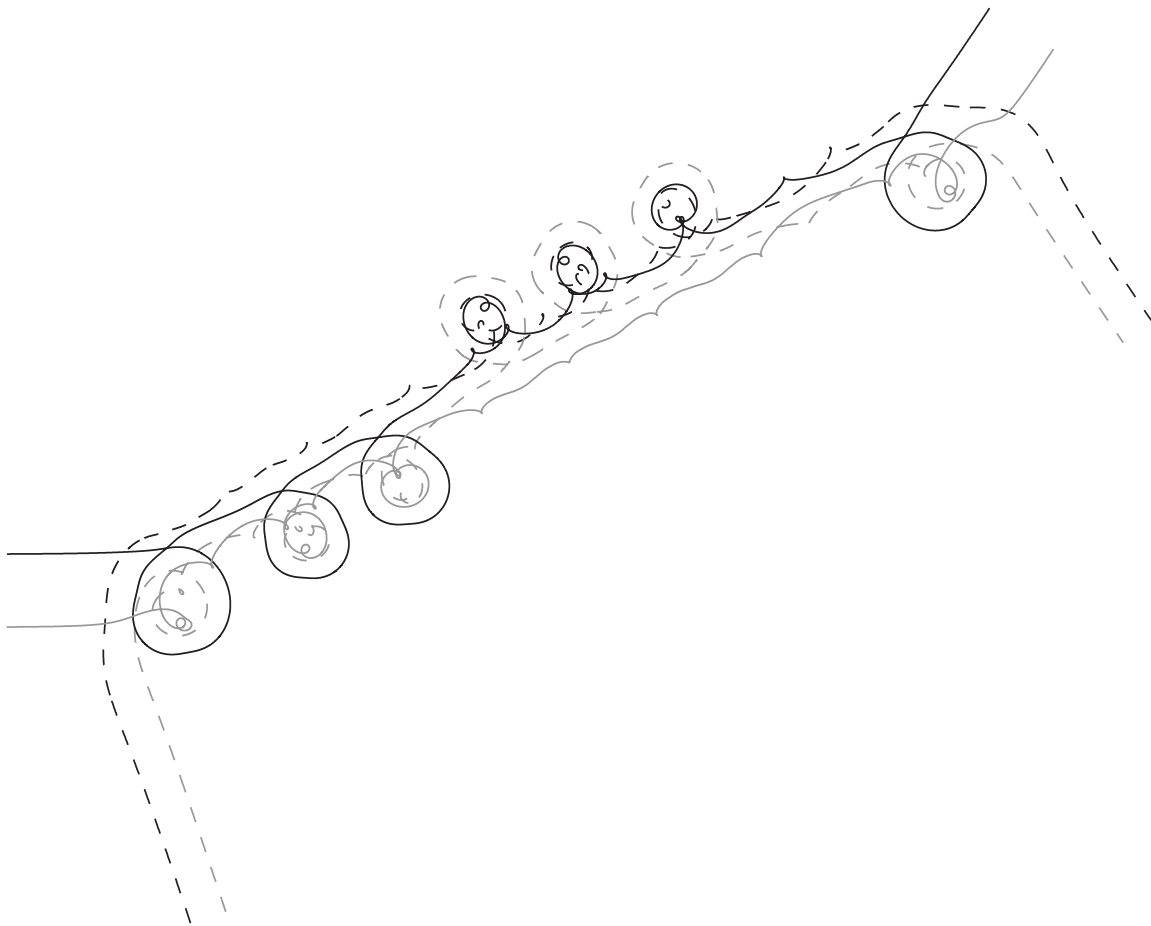


FIG. 7. Scattering of the four-vortex problem into intermediate states that resemble various regimes in the three-vortex problems $(\Gamma, \Gamma, -2\Gamma)$ and $(2\Gamma, -\Gamma, -\Gamma)$. Values for the initial condition are $r=2$, $\Delta=-3\pi/5$, and $\rho \approx 0.819$.

used¹² to classify the various intermediate motions. Either way, strings of finite length are obtained and the chaotic scattering is manifested by the ability to obtain arbitrarily long strings where the length of the string depends sensitively on the initial conditions.

Leapfrogging is an integrable four-vortex motion. One might ask if other integrable cases of four-vortex motion appear as intermediate states during the scattering process. This would require that both X and Y are almost 0. Figure 2(b) provides an example as the reader will see by comparing it to Fig. 13, panel III (IV, V, and VI), of Ref. 14.

III. CONCLUSIONS

A new mechanism for chaotic scattering of two identical point vortex pairs has been found. The mechanism appears as a natural extension of work on the scattering of two vortex pairs with strengths that were close in magnitude but not identical.¹ The new mechanism is distinct from the “sling-shot” mechanism proposed by Price.⁶ It hinges on the apparent existence of unstable motions of the four-vortex system that have periodic relative motion of the four vortices and that resemble solutions to the three-vortex problems $(\Gamma, \Gamma, -2\Gamma)$ and $(2\Gamma, -\Gamma, -\Gamma)$. The four-vortex system approaches such solutions and follows them for a time that depends sensitively on the initial conditions. Taken together, Ref. 1 and

the present work show that the scattering of one vortex pair by another is chaotic for all choices of strengths of the two incoming pairs.

ACKNOWLEDGMENTS

We thank Mark Stremler for helpful comments and constructive criticism. This work was supported by a Niels Bohr Visiting Professorship at the Technical University of Denmark sponsored by the Danish National Research Foundation.

- ¹B. Eckhardt and H. Aref, “Integrable and chaotic motions of four vortices II: Collision dynamics of vortex pairs,” *Philos. Trans. R. Soc. London, Ser. A* **326**, 655 (1988).
- ²S. V. Manakov and L. N. Shchur, “Stochastic scattering,” *Sov. Phys. JETP* **37**, 54 (1983).
- ³H. Aref, J. B. Kadtko, I. Zawadzki, L. J. Campbell, and B. Eckhardt, “Point vortex dynamics: Recent results and open problems,” *Fluid Dyn. Res.* **3**, 63 (1988).
- ⁴G. J. F. van Heijst and J. B. Flór, “Dipole formation and collisions in a stratified fluid,” *Nature (London)* **340**, 212 (1989).
- ⁵O. U. Velasco Fuentes and G. J. F. van Heijst, “Collision of dipolar vortices on the beta plane,” *Phys. Fluids* **7**, 2735 (1995).
- ⁶T. Price, “Chaotic scattering of two identical point vortex pairs,” *Phys. Fluids A* **5**, 2479 (1993).
- ⁷H. Aref, “Motion of three vortices,” *Phys. Fluids* **22**, 393 (1979).
- ⁸N. Rott, “Three-vortex motion with zero total circulation,” *ZAMP* **40**, 473 (1989).

- ⁹H. Aref, "Three-vortex motion with zero total circulation: Addendum," *ZAMP* **40**, 495 (1989).
- ¹⁰W. Gröbli, *Spezielle Probleme über die Bewegung Geradliniger Paralleler Wirbelfäden* (Zürcher und Furrer, Zürich, 1877).
- ¹¹A. E. H. Love, "On the motion of paired vortices with a common axis," *Proc. London Math. Soc.* **25**, 185 (1894).
- ¹²P. L. Boyland, M. A. Stremler, and H. Aref, "Topological fluid mechanics of point vortex motions," *Physica D* **175**, 69 (2003).
- ¹³B. Eckhardt, "Integrable four vortex motion," *Phys. Fluids* **31**, 2796 (1988).
- ¹⁴H. Aref and M. A. Stremler, "Four-vortex motion with zero total circulation and impulse," *Phys. Fluids* **11**, 3704 (1999).